

AD 740144

CHARACTERIZATION OF IR WINDOWS

First Quarterly Technical Report

by

J. S. HAGGERTY, E. T. PETERS

ARTHUR D. LITTLE, INC.

prepared for

OFFICE OF NAVAL RESEARCH
DEPARTMENT OF THE NAVY

sponsored by

ADVANCED RESEARCH PROJECTS AGENCY

MARCH 1972

DDC
RECEIVED
APR 13 1972
C

DISTRIBUTION STATEMENT A
Approved for public release;
Distribution Unlimited

Arthur D. Little, Inc.

The views and conclusions contained in this document are those of the authors and should not be interpreted as necessarily representing the official policies, either expressed or implied, of the Advanced Research Projects Agency or the U.S. Government.

ADDRESS BY			
WFOI	WHITE SECTION	<input checked="" type="checkbox"/>	
DDC	DIFF SECTION	<input type="checkbox"/>	
MANAGEMENT		<input type="checkbox"/>	
JUSTIFICATION			
BY			
DISTRIBUTION/AVAILABILITY STATE			
ORIG.	AVAIL.	NO. 1/2	SPECIAL
A			

FIRST QUARTERLY TECHNICAL REPORT

"Form Approved Budget Bureau No. 22-R0293"

Program Title: Characterization of IR Windows

Contractor: Arthur D. Little, Inc., Cambridge, Massachusetts

Principal Investigator: John S. Haggerty 617-864-5770

**Scientific Officer: Director, Physics Programs
Physical Sciences Division
Office of Naval Research
Department of the Navy**

Contract Number: N00014-72-C-0092

ARPA Order Number: 1806/04-09-71

Program Code Number: S2202A

Effective Date of Contract: 71 October 01

Contract Expiration Date: 72 September 30

Amount of Contract: \$47,533 (plus fee)

**Sponsored by
Advanced Research Projects Agency
ARPA Order No. 1806/04-09-71**

ABSTRACT

Back reflection X-ray topographic techniques have been used to characterize high resistivity GaAs single crystals. The crystals were grown by Bell & Howell under ONR Contract N00014-70-C-0132 and their intended use is for high power IR windows.

Initial results have revealed growth defects as well as defects induced by subsequent processing of the crystals. Strains from faceted growth were evident in most crystals. The surfaces of polished crystal section faces exhibited damage induced during the initial cutting of the crystals as well as during the polishing procedures. It is premature to make any inference that this work damage is in any way responsible for the measured optical absorptivity at $10.6\mu\text{m}$.

Observation of possible point and line defects characteristic of the bulk crystals was not possible with the work damaged surfaces. Procedures to elucidate the degree of bulk crystal perfection will be deferred until the samples have been sectioned and polished in a manner that does not induce work damage.

I. INTRODUCTION

The general status of the absorptivity observed for high resistivity is summarized in Figure 1. ⁽¹⁾ Once high electrical resistivities ($\rho \geq 10^4 \Omega\text{cm}$) are achieved, crystals can be readily grown with optical absorptivities (α) in the range of 0.015 to 0.025 cm^{-1} at 10.6 μm . A few crystals have been prepared that have exhibited α 's slightly below 10^{-2} ; however, they have not been reproduced. Figure 1 summarizes Bell & Howell's history with Cr charge compensation. Approximately the same minimum absorptivity has been observed in crystals compensated with Fe, Ni and undefined charge compensators. The results of absorptivity measurements of crystals previously grown at Arthur D. Little are included to demonstrate how readily GaAs crystals can be produced which fall into this optical absorptivity range. These were the only crystals which we have grown specifically to achieve high resistivities by the use of charge compensating dopants.

The same range of absorptivities can be achieved without adherence to the following intuitively-important parameters. There is no apparent effect on the minimum α despite wide ranges of chemical purity. Most crystals contain 10^{15} to 10^{16} Si atoms per cm^3 ; however, B, O₂, C, Al and F levels can differ by up to two orders of magnitude between individual crystals with no apparent effect on α . The minimum α at 10.6 μm is not affected by the choice of charge compensating dopant as noted above. Absorptivity in GaAs is independent of electrical resistivity when $\rho \geq 10^4 \Omega\text{cm}$. Crystallographic quality has no apparent effect on α . Individual crystals which exhibit widely varying dislocation densities and substructure have the same minimum level of absorptivity at 10.6 μm . The crystal growth technique also appears to have not effect on the minimum α . Both hot wall-

autoclave or liquid-encapsulated Czochralski and horizontal boat grown crystals exhibit the same minimum absorptivity.

These results leave one with two alternatives. Possibly the intrinsic absorptivity of GaAs is of the order of 10^{-2}cm^{-1} at room temperature and $10.6 \mu\text{m}$, although we know of no theoretical reason for this to be so. Alternatively, all of the crystals may contain some common defect which is insensitive to variations in process parameters. We have initiated our characterization program on the basis of the latter hypothesis.

It is well known that chemical homogeneity can be extremely poor on a localized scale in all melt growth III-V semiconductor single crystals. The specific types of defects in GaAs^(2,3) and their causes^(4,5) have been the subject of several review papers and will not be summarized in this report. The essential points are that the growth of heavily doped GaAs single crystals is complicated by a high entropy of fusion, low distribution coefficients, probable retrograde solubility limits over the stoichiometry range and unequal (high) vaporization rates from nominally congruent-melting liquids. These effects can lead to high localized compositional variations, even to the point of exceeding solubility limits with resultant precipitates. The scale of these heterogeneities is generally between tens of angstroms ($\sim 10^{-7} \text{cm}$) to microns ($\sim 10^{-4} \text{cm}$). Thus, they are below the resolution limits of most conventional optical or IR microscopes, in-situ chemical analyses, electrical characterization or optical absorptivity measurements. Our program is designed to search for the presence of localized compositional variations in GaAs, and if detected, to identify their phase chemistry and to calculate their effect on optical absorptivity.

In the initial phase of this program, we will attempt to determine whether any of the probable causes of localized compositional variations is responsible for the persistent residual optical absorptivity at 10.6 μ m. In this initial effort, we will emphasize direct observation techniques (with less emphasis placed on indirect analytical techniques) for determination of the optical absorption mechanism(s) and develop a plan for their use when definitive characterization experiments can be identified. Our emphasis on direct observation techniques stems from the inherent necessity for defining the exact nature of the defect(s) responsible for the residual absorptivity, which is most efficiently done by direct observation and analytical techniques. Precise chemical, structural and morphological definition of defects is necessary so that elimination of the defects causing absorption can be made through modification in crystal growth parameters.

We will begin this analytical program using optical microscopy, transmission and back reflection X-ray topography and transmission electron microscopy techniques for sample characterization. Samples will be secured directly from Bell & Howell, per the terms of our ONR contract, as well as, by direct purchase from other sources.

Under a concurrent ONR-sponsored program, Bell & Howell is striving to prepare high quality, low absorptivity GaAs boules with an eventual goal of achieving diameter scale-up of 3 to 12 inches. In their current phase of work, they are attempting to minimize the absorption coefficient by preparing high quality crystals through selected variation in growth parameters, including dopant, concentration, growth rate, seed orientation, etc. To cover variations in these parameters, they expect to produce

20-25, 1-inch diameter boules from which they will supply to us a 1 cm thick section (including an outside wall and the core) for defect characterization. Bell & Howell will carry out chemical analysis (by spark source mass spectroscopy) and absorption coefficient measurements on each sample supplied. We, in turn, will provide Bell & Howell with the results of our characterization studies which should permit them to optimize crystal growth parameters.

In our preliminary evaluation studies of supplied samples, we have used back reflection X-ray topography as a principal investigative tool. Samples were not received from Bell & Howell until the third month of the contract; thus, we did not have time to initiate transmission electron microscopy and transmission X-ray topographic characterization techniques during the first quarter.

II. CHARACTERIZATION PROCEDURES

Preliminary screening of all as-received GaAs crystals has been carried out by several X-ray methods to provide an estimate of crystallographic perfection and induced surface damage. These screening procedures include a determination of the orientation of all major surfaces by conventional back reflection Laue methods and a measure of structural perfection through wide area Laue patterns and Berg-Barrett (reflection) X-ray topographs.

Wide angle Laues provide a diffraction image from a surface area about 3/8 inch in diameter. Gross crystallographic defects including twins, polygonization, low angle grain boundaries and severe warpage are easily observed. As an example, a wide angle Laue photograph of a (111) GaAs slice containing a twin defect is shown in Figure 2a. Most of the enlarged Laue spots image the defect, indicating that the twinned portion does not satisfy the required diffraction condition as for the rest of the spot; these defect areas reappear at other locations on the pattern. The spot at the top of the pattern, however, is complete; this indicates that the crystallographic plane responsible for this spot corresponds to (or is normal to) the composition plane of the twin defect. For the particular case shown, this spot corresponds to a (112) reflection, and the composition plane of the twin is $(\bar{1}11)$. The wide angle Laue patterns thus provide a very useful tool for qualitative identification of defects at a one-to-one magnification.

On a much finer scale, reflection topographs are capable of revealing defects as small as one micron in extent, including dislocation arrays, precipitates, segregation and so forth. Topographs are obtained through direct X-ray imaging of a selected diffraction plane onto a film.

Although many geometrical and physical factors contribute to the development of a topographic image, the major factor in reflection photographs is the result of strain-induced diffraction contrast, i.e., an increase in the intensity of the diffracted X-ray beam by those regions in the sample that are strained. A very thorough discussion of X-ray topographic procedures, including theory, experimental approach and practical results, has been given by Meieran⁽⁷⁾ and will not be repeated here. Most topographic cameras are designed to achieve a geometrical resolution of about 1 μ m. Since the strain field that is generated around a defect is typically an order of magnitude larger in dimension than the defect itself, in principle, it is possible to observe and specify defects as small as a few tenths of a micron. To utilize the full resolution of the technique, it is necessary to employ high resolution films for image recording, since the photographic image is approximately the same size as the projection of the diffracting plane.

We have found that high speed Polaroid film is suitable for recording a back reflection topographic image in just a few minutes. Besides being of great assistance in carrying out crystal alignment, these images provide greater sharpness than is obtained in the large area Laue patterns. Also, the entire sample can be imaged. As examples, Polaroid reflection topographs of (224) and (440) planes from the GaAs crystal slice containing the twin defect are shown in Figure 2b; as described previously, the (112) reflection does not image the defect.

Topograph resolution is maximized when the diffraction angle is about 90° and when the incident X-ray beam makes a small angle with the surface of the specimen. This geometry is shown schematically in Figure 3. The

point source of X rays is provided by a microfocus X-ray diffraction unit. In most cases, the normal to the sample surface (N) will closely approximate a specific crystallographic direction [hkl]. The X-ray radiation employed is important, for it determines which of the reflection planes can satisfy the condition $2\theta \approx 90^\circ$; furthermore, longer wavelength X rays are more easily absorbed by the specimen material. As an example, 80% of the diffracted intensity from GaAs occurs from the first $4\mu\text{m}$ for CrK_α radiation, but from the first $10\mu\text{m}$ for CuK_α radiation (see Figure 4). A topograph obtained with CrK_α radiation would therefore be more sensitive to surface preparation.

Work to date has been carried out with CuK_α radiation ($\lambda = 1.54051\text{\AA}$). Reflections which fulfill the condition $2\theta \approx 90^\circ$ include (422), (333), (511) and (440). Available reflection conditions for typical surface plane orientations are as follows:

<u>Reflection Plane</u>	<u>$2\theta_{\text{CuK}_\alpha}$</u>	<u>Surface Plane</u>	<u>ϕ (see Figure 3)</u>
(422)	83.7°	(111)	22.4°
		(110)	11.9°
		(211)	8.4°
(333)	90.1°	(111)	45.1°
		(110)	9.8°
		(211)	25.6°
(511)	90.1°	(111)	6.1°
		(110)	8.3°
		(211)	6.8°
(440)	100.8°	(111)	14.9°
		(110)	50.4°
		(211)	20.4°

The (422) reflection has been used for all screening experiments, since the relative intensity of this reflection is about three times that of (440) or (551) planes and six times that of (333); as a result, exposure times are reduced with little sacrifice in resolution. The (511) reflection has been employed in some cases to evaluate the exposure and processing of high resolution plates.

Topographic diffraction images have been recorded on three types of films; alignment shots are recorded on Polaroid Type 57, low resolution (up to 20X enlargement) on Kodak Xo Screen medical film, and high resolution (up to 150X enlargement) on Ilford L4 plates, 50 μ m emulsion thickness. Typical exposure times are (for CuK_α radiation, (422) reflection, 35 kV, 3 ma):

Polaroid - 1 minute

Xo Screen - 40 minutes

L4 - 6 hours

Film processing, especially in the case of high resolution plates, is very exacting and requires a great deal of care to avoid artifacts on the plates which might be erroneously interpreted as defects in the crystals. The procedure given by Meieran⁽⁷⁾ for processing nuclear plates is typical and should give good results. It is imperative that water be very pure (high resistivity, triply distilled, deionized) and filtered to prevent plate contamination during processing. We are in the process of evaluating several procedures for film processing, printing and enlarging and will provide the approach we feel is best at a later time.

III. RESULTS OF CHARACTERIZATION PROGRAM

1. Description of Samples

The samples received to date from Bell & Howell are listed in Table I. These samples were all about 1 cm thick sections with the growth axis, which is $\langle 111 \rangle$ in all cases, coinciding with the normal to the section plane. Section surfaces were polished to a good optical finish for purposes of measuring the absorption coefficient; optical microscopy revealed no evidence of surface defects remaining from polishing. In addition, each of the samples contained a flat along the side which corresponded closely to a (211) plane.

Table I also lists two samples purchased from commercial sources. Acceptance specifications for these samples were:

Cr-doped to a resistivity greater than 10^6 ohm-cm

Cube 1 cm on edge with a cube edge along direction of growth

Growth direction to be identified.

Both samples were obtained from $\langle 111 \rangle$ grown Czochralski boules and had faces close to (111), (110) and (211) planes.

2. Results

Laue patterns were taken on each of the samples listed in Table I to determine reference plane orientations. In addition, wide angle Laue patterns were obtained from arbitrary "center" and "periphery" positions on each of the Bell & Howell samples and from three mutually perpendicular faces on the two cubes. There were no gross defects,

such as twins or polygonization (low angle boundaries), observed in any of the samples. Some structure was noted in the wide angle Laues of one of the cubes, which was attributed to surface damage introduced during sawing and grinding.

A series of low magnification (422) reflection topographs for these specimens are presented in Figures 4 to 13. A discussion of the observed surface defects for each of the samples follows:

Sample 1852T (Figures 5 to 7)

Crystal warpage is evident in the low magnification topograph (Figure 5) by the variation in background contrast. In addition, damage resulting from scratches due to handling are abundant. The severe damage indicated by A (Figure 5) was probably the result of sliding over a particle of grit in the sample box. The broad bands marked B are the result of a spurious X-ray reflection and should be ignored. The light bands C, probably result from damage induced during the initial cutting process.

Surface damage resulting from polishing scratches is exhibited in Figures 6 and 7. Optical examination of these areas shows very smooth, well polished surfaces. The apparent scratch marks on the topographs are the result of below-the-surface deformation remaining from the polishing operation. The light band A (Figure 6) is similar to the bands designated C in Figure 5. The small black dots are defects in the film emulsion; studies are being carried out to avoid these kinds of defects. It is clear that the polishing procedures employed with these crystals induced extensive surface damage. The damage is so severe that it obscures defects characteristic of the bulk crystal. We will repolish sections of these samples for use in back reflection and transmission X-ray

topographic characterization of bulk defects.

Sample 1857T (Figure 8)

Background is quite uniform, but with evidence of scratches and other surface damage due to specimen handling. There is an indication of specimen warpage and strain along sample radials spaced 120° apart; these areas are indicated by arrows. The strain damage is the result of faceted crystal growth.

Sample 1860T (Figure 9)

This sample is much like the previous sample, but strain due to faceting is much more in evidence, as indicated by arrows. The defect A is a hole in the emulsion of the X-ray plate.

Sample 1860B (Figures 10 and 11)

This is a section from the bottom (i.e., the last to freeze portion) of the same boule from which the preceding sample was obtained. Strain induced by faceted growth is much more prominent and results in substantial crystal deformation. Propagation of this defect through the thickness of the sample is shown by Figure 11, a topograph of the other side of the sample. The light area in the upper right corner is the result of a chip out of the crystal which probably occurred during cutting or polishing.

Sample 2602-10 (Figure 12)

The boule from which this sample was obtained was grown by liquid encapsulation. The sample section shows no evidence for faceting and macroscopically represents the best quality crystal out of the lot of Bell & Howell samples examined. Considerable surface damage due to sample handling and polishing is in evidence; this damage could be removed by appropriate polishing.

Commercial Samples

A series of (422) reflection topographs were obtained from (111), (110), and (211) as-cut faces of the two GaAs cubes obtained commercially. These topographs are presented in Figures 13 and 14. The cube from Commercial Source A produces generally uniform topographs. The sample appears to have good perfection, with only slight evidence of residual saw damage, evident on the (111) face. The chip on the corner resulted from dropping the crystal. In contrast, the sample from Commercial Source B reveals considerable structure which we attribute to massive damage from high speed sawing. As a result of this extensive damage, it is not possible to comment on the sample's crystallographic and microstructural quality. It is evident that the damage induced during the initial sawing extends deep into the crystal. Many of the Bell & Howell crystals exhibit similar residual damage of this type on polished surfaces.

These samples will be used for evaluating and developing our own sawing and polishing procedures.

3. Summary of Characterization Results

The low-magnification, macroscopic back reflection X-ray topographs of the five Bell & Howell samples has revealed significant differences in residual stress resulting from growth conditions. One crystal (1860B) was highly stressed; two were moderately stressed (1857T and 1860T) and two were essentially free of stresses induced from growth faceting (1852T and 2602-10). Typical of the anomalies which have appeared in determining the cause of the optical absorptivity, one of the best crystals from the point of structural perfection (1852T) had the highest absorptivity (0.031 cm^{-1}) at 10.6μ .

IV. FUTURE WORK

During the second quarter of this program, we will continue to characterize these and other samples which we expect to receive from Bell & Howell. Surface damage areas will be removed to permit characterization of bulk point and line defects in the crystals. Sections will also be thinned to approximately 1000\AA to permit characterization of the samples by transmission electron microscopy.

The usefulness of IR microscopy will be investigated. Preliminary results with microscopes operating at approximately $1\mu\text{m}$ wavelength have provided some interesting insights. Stress fields corresponding to the strain fields in the X-ray topographs resulting from growth faceting were visible in polarized transmitted light. This indicates that the crystals still contain residual stresses as well as strained areas. Because the low wavelength absorption edge is shifted upward, the usefulness of $1\mu\text{m}$ illumination is somewhat compromised for Cr-doped GaAs.⁽³⁾ Thick samples appeared quite opaque, and overlapping defects could not be easily resolved.

Processing and exposure conditions for the high resolution X-ray plates will continue to receive attention. The topograph images are essentially the same scale of size as are the samples; thus, all magnified observations must be made on the high resolution plates. Care must be taken to insure that defects in the crystal are observed. Dust, for example, presents a serious problem in handling the plates. Also, plate processing conditions must assure minimum grain growth of the silver to yield maximum resolution. When the Ilford L4 plates are exposed to optical photons, they can be usefully magnified in excess of 1000 times. To date, the grain size

in the same plates exposed to X-ray radiation has not permitted magnification in excess of 300 times. We intend to determine whether this is inherent to the interactions of X rays with AgBr emulsions or whether grain-size growth can be prevented by modified film processing procedures.

V. REFERENCES

1. "Development of GaAs Infrared Window Material," Bell & Howell
Technical Summary Report, December 1970, Contract N00014-70-C-0132.
2. E. S. Meieran, Trans TMS-AIME, 242:413 (1968).
3. E. D. Jungbluth, Met. Trans., 1:575 (1970).
4. a. A. F. Witt, J. Elect. Chem. Soc., 144:298 (1967).
b. K. Marizane, A. F. Witt and H. C. Gatos, J. Elect. Chem. Soc.
144:738 (1967)
5. R. M. Logan and D. T. J. Hurle, J. Phys. Chem Solids, 32:1739 (1971).
6. J. S. Haggerty and E. T. Peters, Conference on High Power Infrared
Laser Window Materials, Oct. 27-28, 1971, Ed.; C. S. Sahagian
and C. A. Pitha, p. 121.
7. E. S. Meieran, Siemens Review XXXVII (1970) Fourth Special Issue
"X-ray and Electron Microscopy," p. 39.

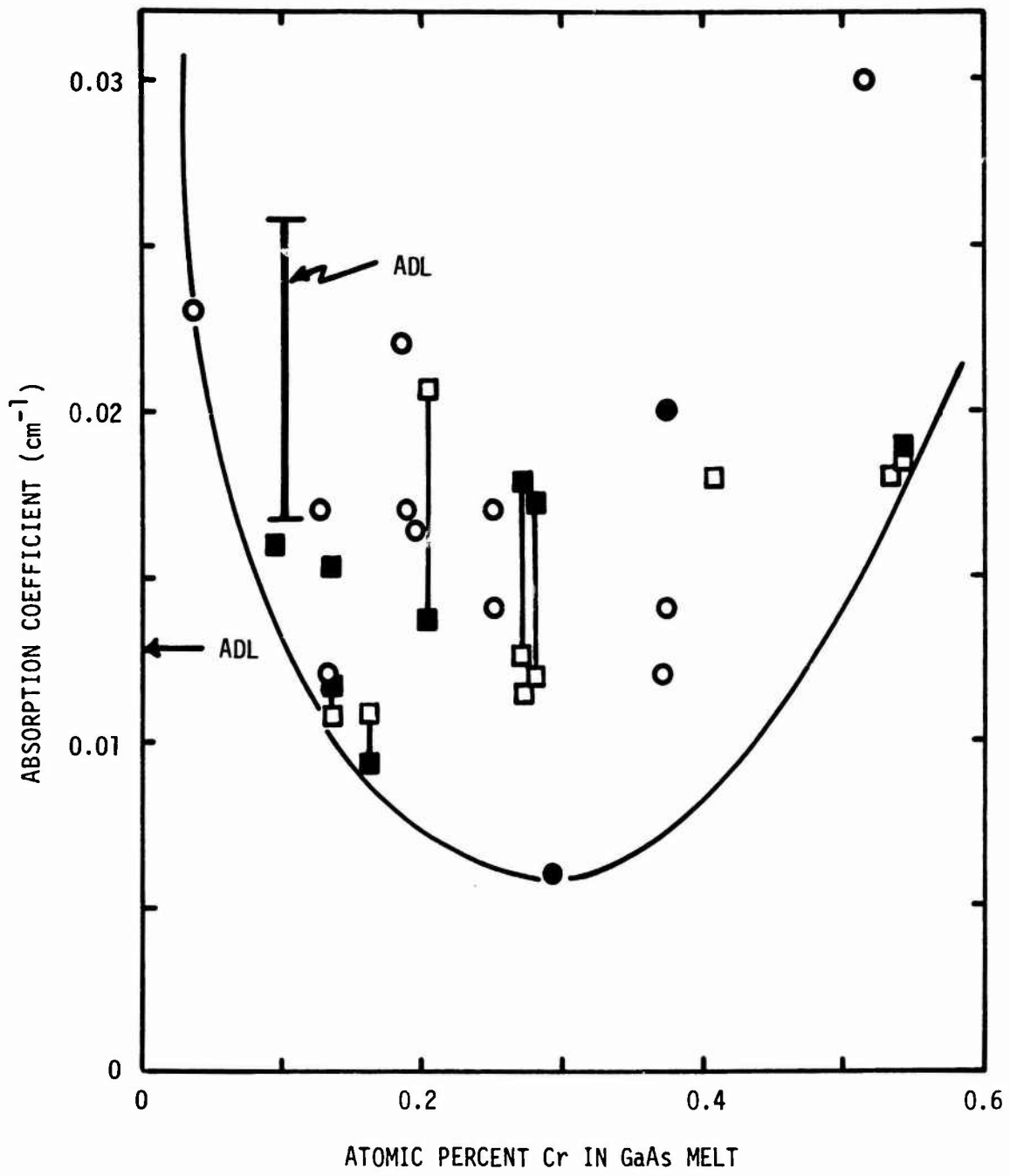
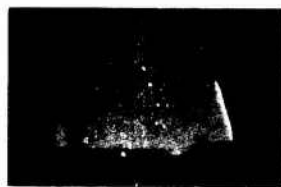


FIGURE 1 THE ABSORPTION COEFFICIENT OF Cr-DOPED GaAs AT 10.6 MICRONS AND 300°K AS A FUNCTION OF THE CHROMIUM CONCENTRATION IN THE INITIAL MELT



Reproduced from
best available copy.

a) Wide Angle Laue



(422)



(440)

b) Reflection Topographs, 1X

FIGURE 2 DEMONSTRATION OF THE PRESENCE OF A GROWTH TWIN DEFECT IN A (111) GaAs SLICE

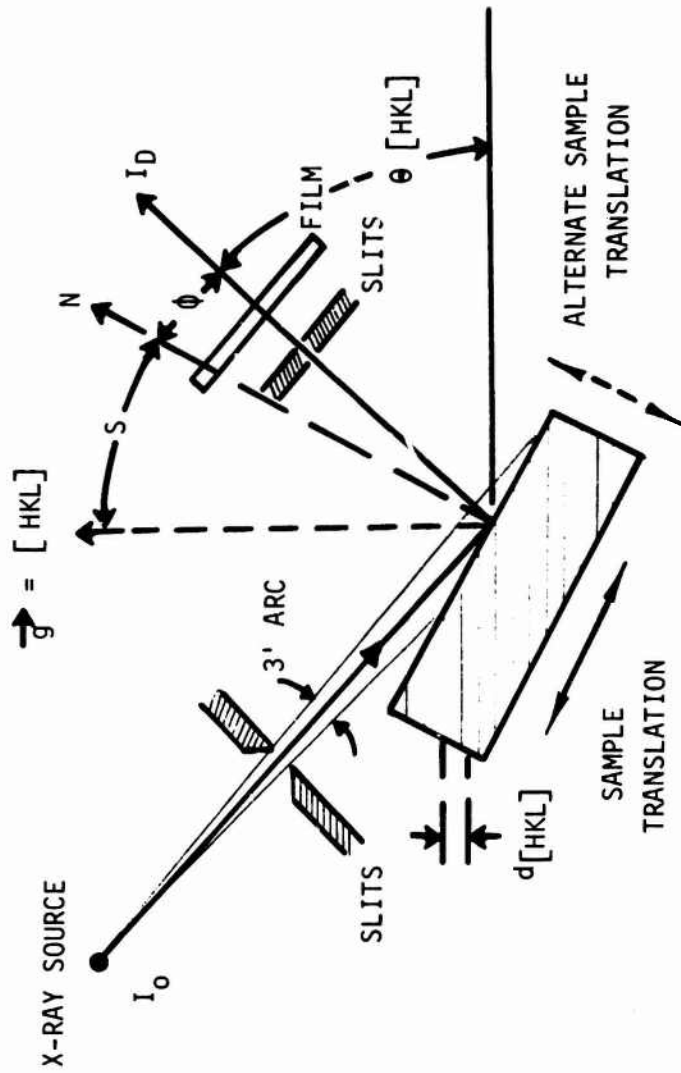


FIGURE 3 SCHEMATIC SKETCH SHOWING THE ASYMMETRICAL SCANNING REFLECTION TOPOGRAPHY GEOMETRY

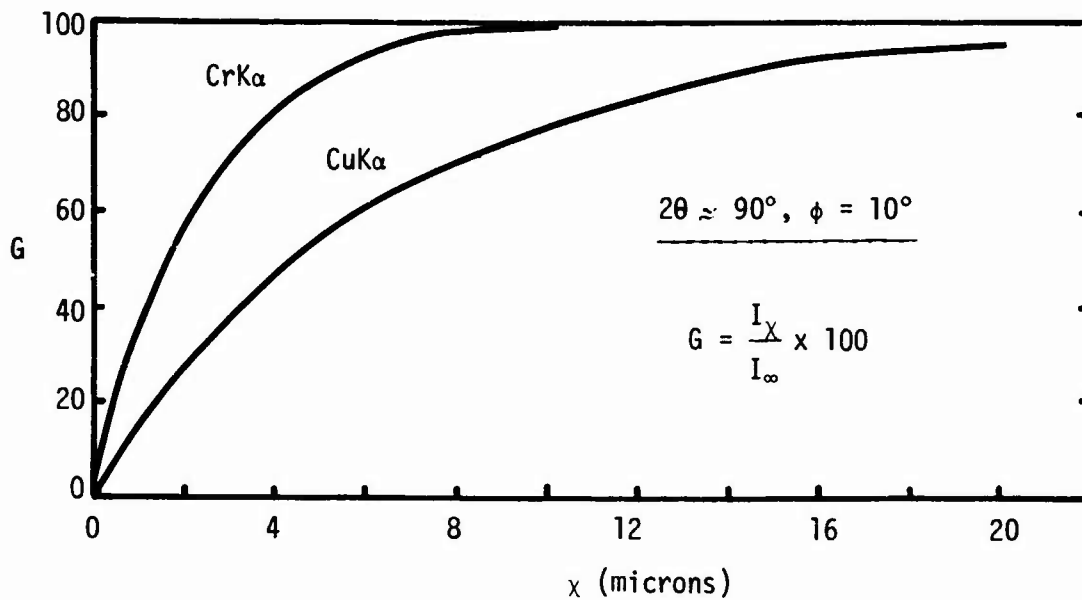


FIGURE 4 PERCENT OF DIFFRACTED BEAM INTENSITY FROM SURFACE LAYER OF THICKNESS x COMPARED TO INTENSITY FROM INFINITELY THICK SAMPLE



FIGURE 5 (422) REFLECTION TOPOGRAPH OF SAMPLE 1852T, 6X



FIGURE 6 (422) REFLECTION TOPOGRAPH OF SAMPLE 18327, 14.5X

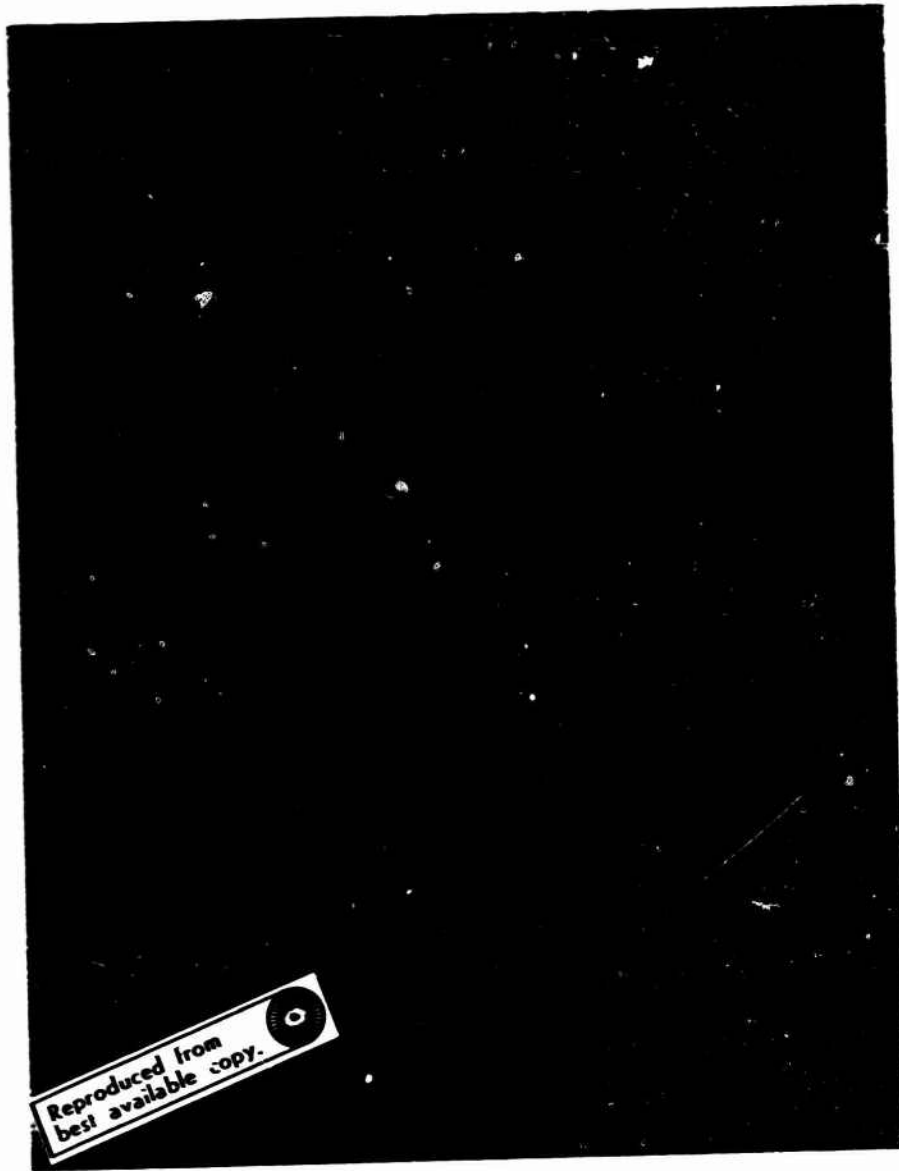


FIGURE 7 (422) REFLECTION TOPOGRAPH OF SAMPLE 1852T, 30X



FIGURE 8 (422) REFLECTION TOPOGRAPH OF SAMPLE 1857T, 6.5X



FIGURE 9 (422) REFLECTION TOPOGRAPH OF SAMPLE 1860T, 6.2X

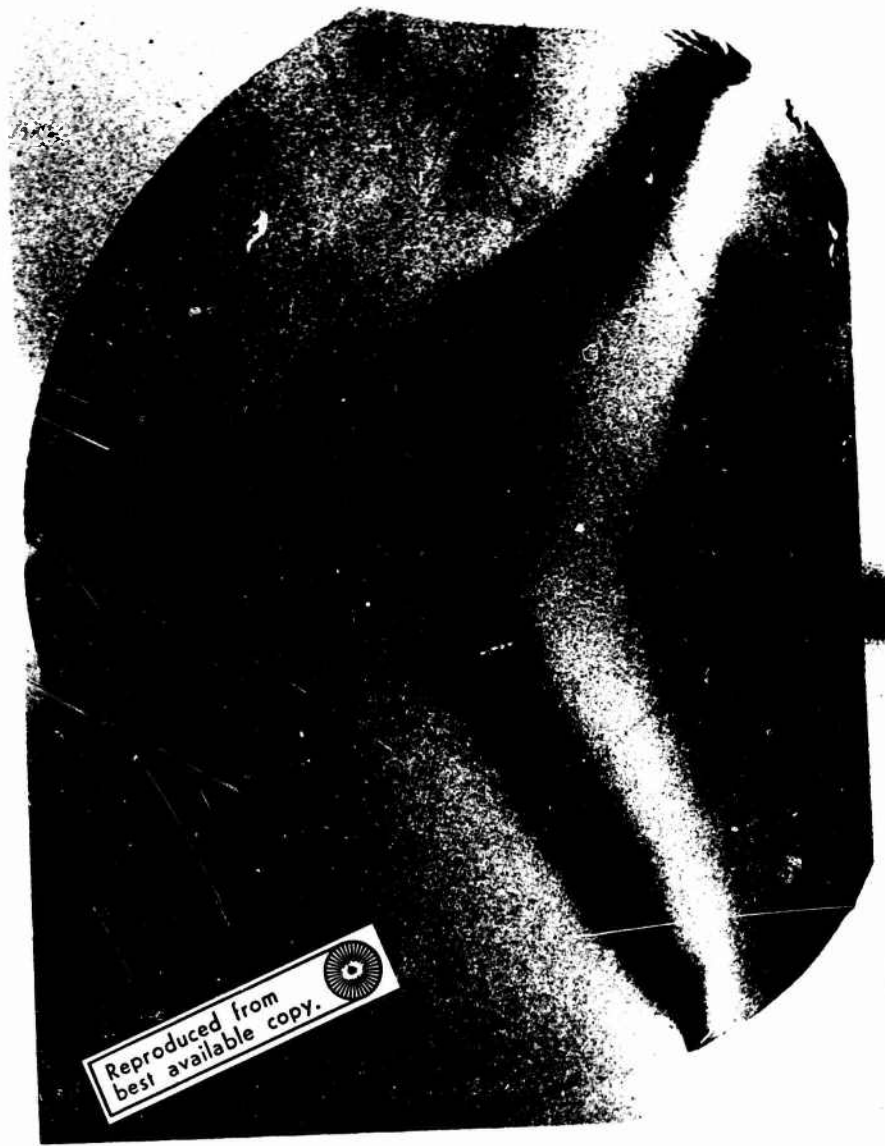


FIGURE 10 (422) REFLECTION TOPOGRAPH OF SAMPLE 1860B (front), 6.2X



FIGURE 11 (422) REFLECTION TOPOGRAPH OF SAMPLE 1860B (back), 6.2X

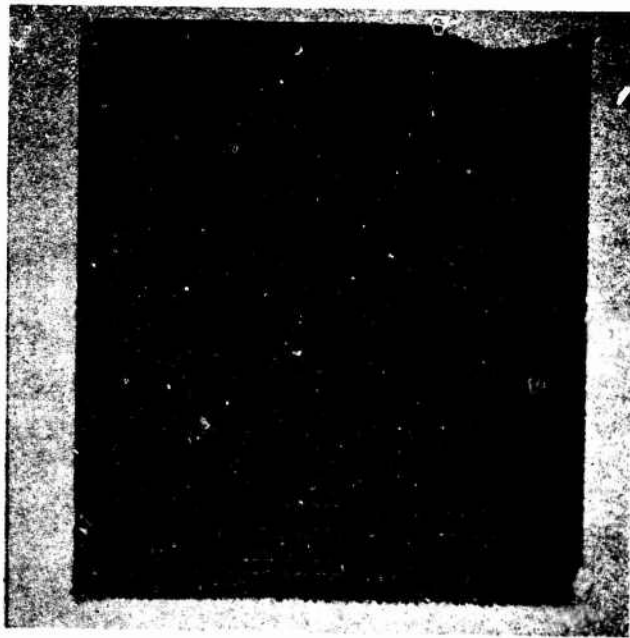


FIGURE 12 (422) REFLECTION TOPOGRAPH OF SAMPLE 2602-10, 10.5X

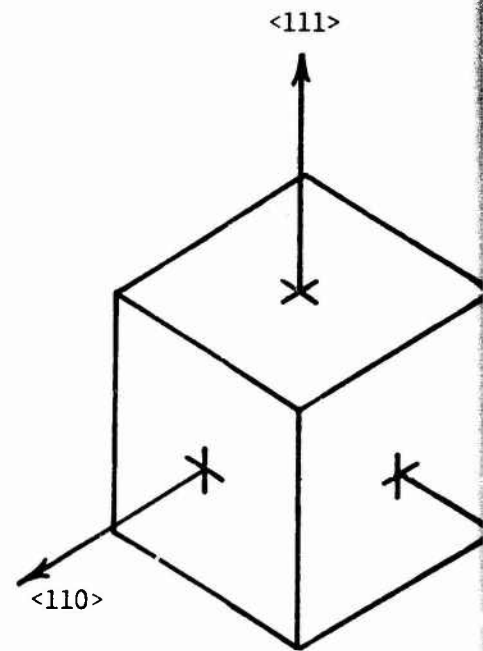
Reproduced from
best available copy.



$\langle 111 \rangle$



$\langle 110 \rangle$



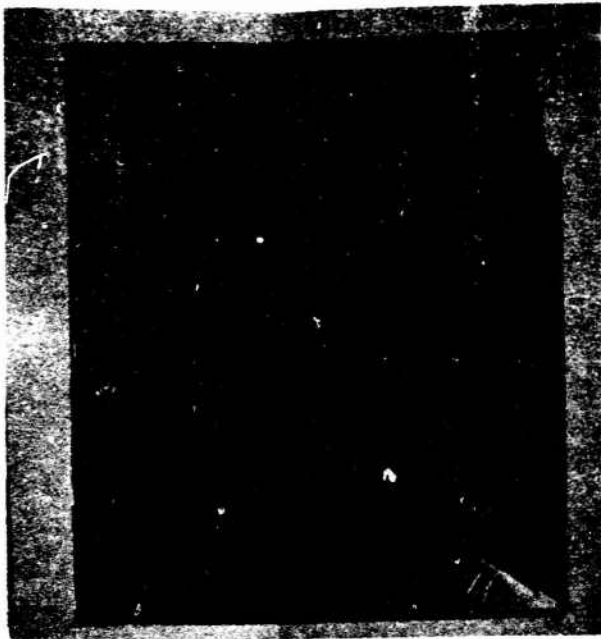
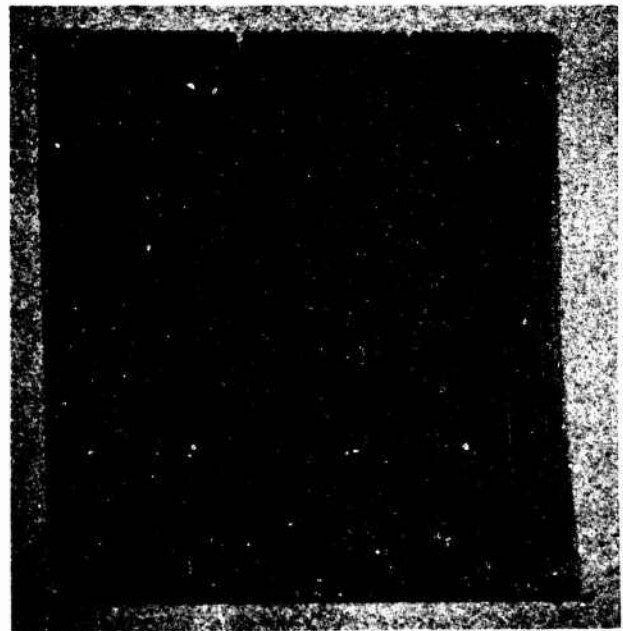
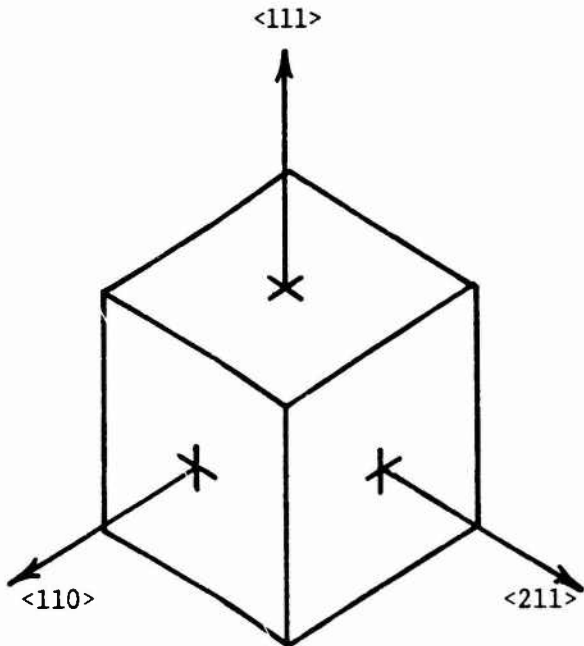


FIGURE 13 (422) REFLECTION TOPOGRAPHS
OF 1 CM CUBE OF GaAs FROM
COMMERCIAL SOURCE A, 10X

$\langle 111 \rangle$



$\langle 211 \rangle$

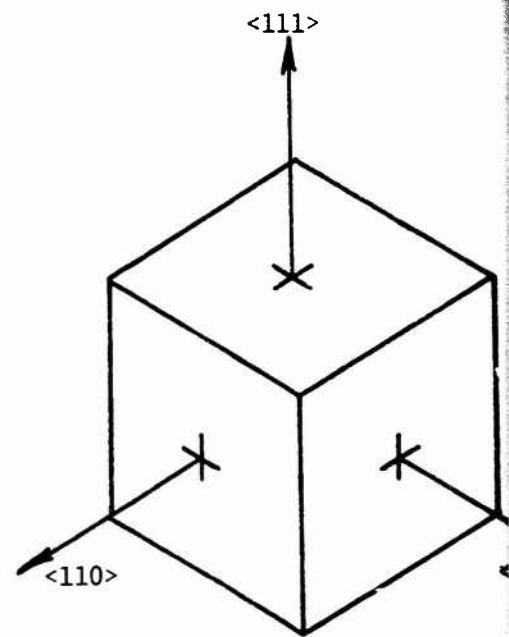


$\langle 111 \rangle$

Reproduced from
best available copy.



$\langle 110 \rangle$



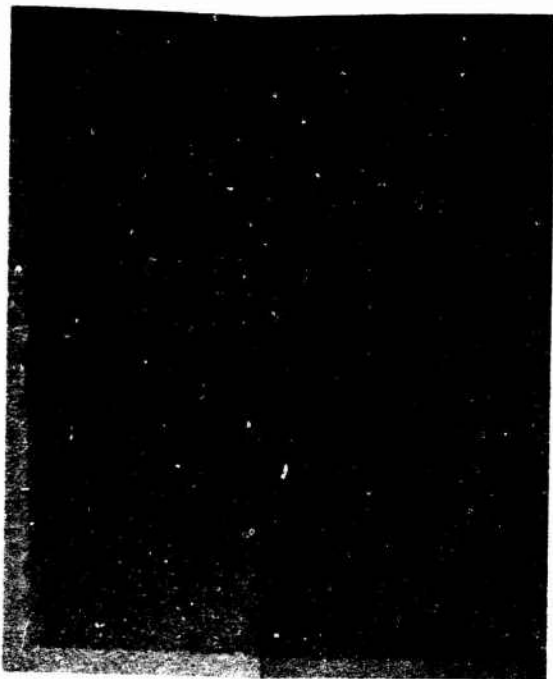
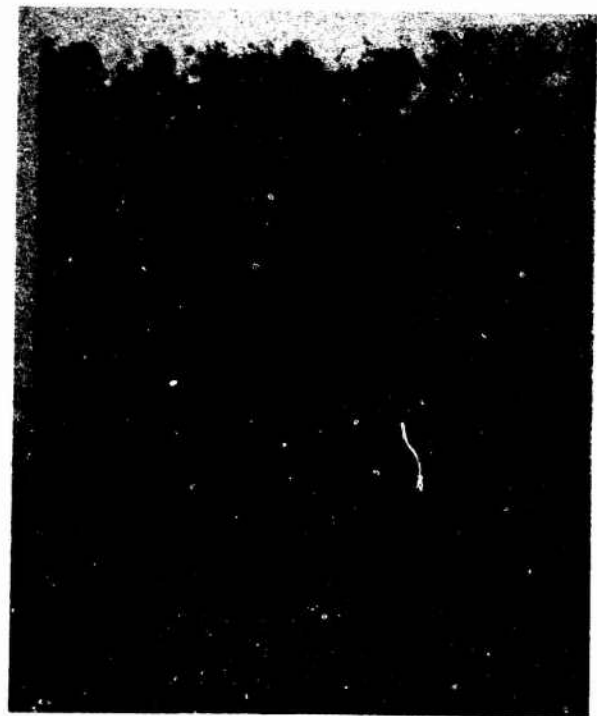
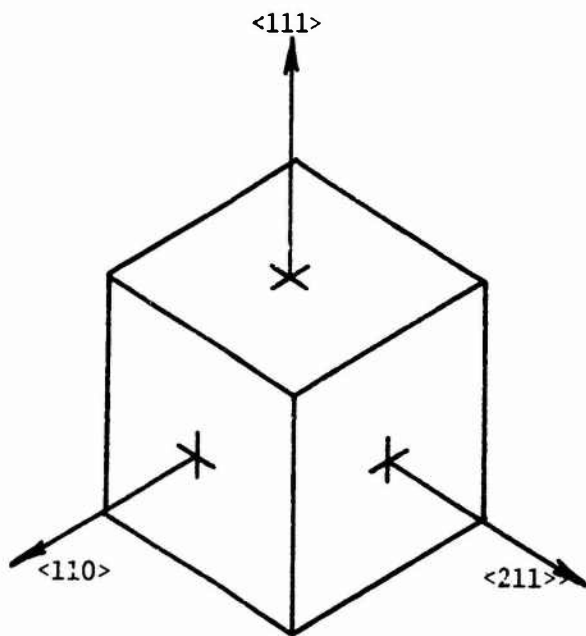


FIGURE 14 (422) REFLECTION TOPOGRAPHS
OF 1 CM CUBE OF GaAs FROM
COMMERCIAL SOURCE B, 10X

$\langle 111 \rangle$



$\langle 211 \rangle$